

# Generation mechanism and interpretation of attenuation band of VLF-saucers

A K Gwal

Department of Physics, Bhopal University, Bhopal 462 026

and

Manjesh Singh

M.P. Council of Science & Technology, Maharana Pratap Nagar, Bhopal 462 011

and

R E Horita

Department of Physics, University of Victoria, Victoria, British Columbia V8W2Y2, Canada

Received 14 June 1988; accepted 30 December 1988

An analysis of the ISIS-VLF data detected by magnetometer in the auroral region of the magnetosphere has been carried out for VLF-saucers. The generation mechanism of VLF-saucers has been studied in terms of excitation of electrostatic cyclotron harmonic emissions due to energetic ions and electrons in the magnetospheric plasma. The attenuation bands of VLF-saucers, as observed by ISIS-2 satellite, have been discussed and it is interpreted that the cyclotron absorption of low energy protons at harmonics of local proton-cyclotron frequencies may be the cause for attenuation bands in VLF-saucers.

## 1 Introduction

VLF-saucers were first observed with the Canadian Satellites Alouette 1 and 2 and have been observed for many years in the auroral ionosphere by various satellites carrying VLF radio receiver<sup>1-4</sup>. The saucers can be observed along the auroral field lines from the plasmopause around 75° latitude and they are known to possess a V-shaped or a hyperbola-shaped dynamical spectral pattern. The height at which they are observed is usually 1000-3000 km, and the width of a saucer is 10-100 km in latitude. Saucers exhibit attenuation bands related to the proton-cyclotron frequency<sup>1,5</sup>. Smith<sup>1</sup> has observed the noise bands at the centre of a saucer with distinct intensity minima at the local cyclotron harmonic frequency.

Klumper<sup>6</sup> also noted that VLF-saucers show absorption bands in the frequency-time spectrogram at the integral multiples of the proton-cyclotron frequency. Horita and James<sup>7</sup> have discussed in detail about the source regions of VLF-saucers from attenuation bands observed at the local cyclotron frequencies and their regions are due to upgoing whistler mode waves.

In the present paper, the occurrence of saucers and the observed attenuation bands on them have been discussed on the basis of the excitation of electrostatic electron and ion-cyclotron harmonic waves in the magnetosphere<sup>8</sup>. A generalized dispersion relation

has been considered for the electrostatic waves propagating at large angles with respect to the magnetic field in a non-Maxwellian anisotropic hot beam-magnetoplasma. The study of the growth rate of electron-cyclotron harmonic (ECH) wave has been incorporated and discussed with reference to temperature anisotropy. As the temperature anisotropy increases, the growth rate increases<sup>9</sup>. Importance of this study has been indicated for the generation of electrostatic whistler waves in presence of the electron beam<sup>3</sup>. These waves in upgoing trend may be responsible for the generation of the saucers in the auroral region of the magnetosphere. Similar study has been carried out for the damping of the electrostatic ion-cyclotron harmonic (ICH) wave. Assuming ions to be protons, the damping of the ion-cyclotron waves at the harmonics of proton-cyclotron frequency may explain the attenuation band in VLF-saucers<sup>10</sup>. Selected ISIS-VLF data detected by magnetometer have been taken for different events, and growth and damping of the waves have been calculated. The results thus obtained have been discussed in terms of occurrence and attenuation band of saucers.

## 2 Theoretical considerations

The dispersion relation for a hot beam-magnetoplasma system under electrostatic approximation may be written as:

$$D = 1 + \varepsilon_e + \varepsilon_b = 0 \quad \dots (1) \quad \lambda_{\parallel b} = k_{\parallel} \rho_{\parallel b}$$

where  $\varepsilon_e$  and  $\varepsilon_b$  are susceptibilities of the electron and the beam and are expressed as<sup>11</sup>:

$$\varepsilon_e = 1 + \sum_{n=-\infty}^{\infty} \frac{2\omega_{pe}^2}{k^2 V_{Te}^2} I_n(\lambda_{\perp e}) e^{-\lambda_{\perp e}} \\ \times \left[ \frac{n}{(x_e + n)} - \frac{1}{2} \left( \frac{T_{\perp}}{T_{\parallel}} \right)_e \frac{\lambda_{\parallel e}}{(x_e + n)^2} \right] \\ + \frac{i\sqrt{\pi} e^{-\alpha_{ne}}}{\sqrt{\lambda_{\parallel e}}} [(x_e + n)(T_{\perp}/T_{\parallel})_e - n]$$

$$\varepsilon_b = 1 + \sum_{m=-\infty}^{\infty} \frac{2\omega_{pb}^2}{k^2 V_{T_{\perp b}}^2} I_m(\lambda_{\perp b}) e^{-\lambda_{\perp b}} \\ \times \left[ \frac{m}{(x_e + m - k_{\parallel} \rho_{db})} \right. \\ \left. - \frac{1}{2} \left( \frac{T_{\perp}}{T_{\parallel}} \right)_b \frac{\lambda_{\parallel b}}{(x_e + m - k_{\parallel} \rho_{db})^2} \right] \\ + \frac{i\sqrt{\pi}}{\sqrt{\lambda_{\parallel b}}} e^{-\alpha_{mb}} [(x_e + m - k_{\parallel} \rho_{db})(T_{\perp}/T_{\parallel})_b - m]$$

where

$$k^2 = k_{\perp}^2 + k_{\parallel}^2 \quad \text{Propagation vector}$$

$$\omega_{ps} = \left( \frac{Ne^2}{\varepsilon_0 m_s} \right)^{1/2} \quad \text{Plasma frequency}$$

$$\Omega_s = (eB_0/m_s) \quad \text{Angular cyclotron frequency}$$

$$V_{T_{\perp s}} = (2T_{\perp s}/m_s)^{1/2} \quad \text{Thermal velocity across the magnetic field}$$

$$V_{T_{\parallel s}} = (2T_{\parallel s}/m_s)^{1/2} \quad \text{Thermal velocity along the magnetic field}$$

$$V_{db} \quad \text{Drift velocity of beam}$$

$$T_{\perp s} \quad \text{Thermal energy across the magnetic field}$$

$$T_{\parallel s} \quad \text{Thermal energy along the magnetic field}$$

$$\lambda_{\perp e} = \frac{1}{2} k_{\perp}^2 \rho_{\perp e}^2; \quad \alpha_{ne} = \frac{\omega - n\Omega_e}{k_{\parallel} V_{Te}}$$

$$\lambda_{\parallel e} = k_{\parallel} \rho_{\parallel e}$$

$$\lambda_{\perp b} = \frac{1}{2} k_{\perp}^2 \rho_{\perp b}^2; \quad \alpha_{mb} = \frac{\omega - m\Omega_e - k_{\parallel} \rho_{db}}{k_{\parallel} V_{T_{\parallel b}}}$$

$$\rho_{db} = V_{db}/\Omega_e$$

$$x_e = \omega/\Omega_e$$

s Species of the particles (i.e., s = e, b)

$\perp$  and  $\parallel$  Directions perpendicular and parallel to the background magnetic field

$I_n$  and  $I_m$  Modified Bessels functions of  $n$ th and  $m$ th order

Here the ambient electrons have an anisotropic Maxwellian velocity distribution with an inequality  $T_{\perp} > T_{\parallel}$ , whereas the beam electrons have a distribution of the same shape but shifted by an amount  $V_{db}$  in the magnetic field direction. Now substituting the values of  $\varepsilon_e$  and  $\varepsilon_b$  in Eq. (1) and separating the imaginary part of  $D$  in order to get growth/damping rate, we follow<sup>12</sup>

$$\frac{\gamma_s}{\Omega_s} \Big|_{s=e,b} = - \left( \frac{\pi}{2} \right)^{1/2} \frac{A_1 + B_1}{C_1} \quad \dots (2)$$

where

$$A_1 = \frac{e^{-\alpha_{ne}}}{\sqrt{\lambda_{\parallel e}}} I_n(\lambda_{\perp e}) e^{-\lambda_{\perp e}} \left[ (x_e + n) \left( \frac{T_{\perp}}{T_{\parallel}} \right)_e - n \right]$$

$$B_1 = \frac{e^{-\alpha_{mb}}}{\sqrt{\lambda_{\parallel b}}} I_m(\lambda_{\perp b}) e^{-\lambda_{\perp b}} \left[ (x_e + m) \left( \frac{T_{\perp}}{T_{\parallel}} \right)_b - m \right]$$

$$C_1 = I_n(\lambda_{\perp e}) \exp(-\lambda_{\perp e}) X_1 \\ + M_1 Y_1 I_m(\lambda_{\perp b}) \exp(-\lambda_{\perp b})$$

$$M_1 = \frac{\omega_{pb}^2}{\omega_{pe}^2} \cdot \frac{V_{T_{\perp e}}^2}{V_{T_{\perp b}}^2}$$

$$X_1 = \frac{1}{\lambda_{\parallel e}} \left[ n - 2(x_e + n)(T_{\perp}/T_{\parallel})_e - \frac{n(x_e + n)^2}{\lambda_{\parallel e}} \right]$$

$$Y_1 = \frac{1}{\lambda_{\parallel b}} \left[ m - 2(x_e + m - k_{\parallel} \rho_{db})(T_{\perp}/T_{\parallel})_b \right. \\ \left. - \frac{m(x_e + m - k_{\parallel} \rho_{db})^2}{\lambda_{\parallel b}} \right]$$

and

$$\frac{\gamma_s}{\Omega_s} \Big|_{s=e,b} = \left( \frac{\pi}{2} \right)^{1/2} \frac{A_1 + B_1}{D_1} \quad \dots (3)$$

where

$$D_1 = I_n(\lambda_{\perp e}) \exp(-\lambda_{\perp e}) X_2 \\ + M_1 Y_2 I_m(\lambda_{\perp b}) \exp(-\lambda_{\perp b})$$

$$X_2 = \frac{n}{x_e + n} + 2 \left( \frac{T_{\perp}}{T_{\parallel}} \right)_e \frac{\lambda_{\parallel e}}{(x_e + n)^3}$$

$$Y_2 = \frac{m}{(x_e + m - k_{\parallel} \rho_{db})} + 2 \left( \frac{T_{\perp}}{T_{\parallel}} \right)_b \frac{\lambda_{\parallel b}}{(x_e + m - k_{\parallel} \rho_{db})^3}$$

Eqs (2) and (3) give the expressions for growth and damping rate of the electrostatic cyclotron harmonic waves in presence of beam<sup>3</sup>. Computations have been carried out for the growth and damping rate of these waves for different plasma parameters obtained from ISIS-2 satellite during the occurrence of VLF-saucers events. A detailed discussion on observational data for the generation mechanism of VLF-saucers and interpretations of the attenuation bands has been incorporated.

### 3 Observational data

Fig. 1 shows the VLF-spectrogram exhibiting a number of saucers. The ISIS-VLF data for this event on 13 Feb. 1974 at 0314 : 07 hrs UT have been considered for the computations of the growth rate of the electrostatic electron cyclotron wave in presence of beam (electrostatic whistler wave) for different temperature anisotropies of the beam electrons. Fig. 2 shows the resonant wave growth that occurs at  $\omega = \Omega_e$  and that increases with the increase of the anisotropy,  $(T_{\perp}/T_{\parallel})_b$ . The growing electrostatic whistler mode in upgoing trend may be one of the causes for the generation of VLF-saucers as observed for the above event.

The damping rate of ICH waves at the harmonics of the proton-cyclotron frequency has been computed for the plasma parameter from ISIS-VLF data for the event on 27 Nov. 1971 at 0418 : 32 hrs UT (Fig. 3) and plotted in Fig. 4 which shows that ICH waves are damped either at  $(m + 1)\Omega_p$  for lower temperature

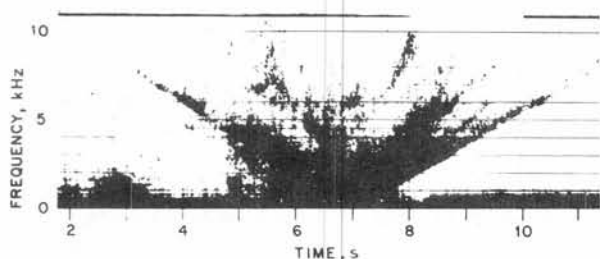


Fig. 1—ISIS-2 satellite spectrogram (0-10 kHz) showing the saucer [satellite height = 1367 km (66.9°N; 9.8°E Geomagn)]

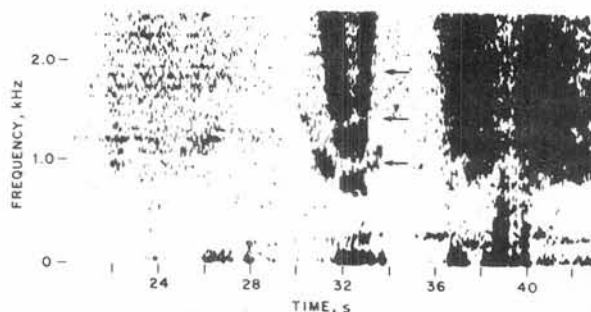


Fig. 3—ISIS-2 satellite spectrogram (0-2.5 kHz) showing the saucer [The three arrows point to the attenuation bands related to the proton-cyclotron frequency, satellite height = 1428 km (68.1°N; 16.4°E Geomagn)]

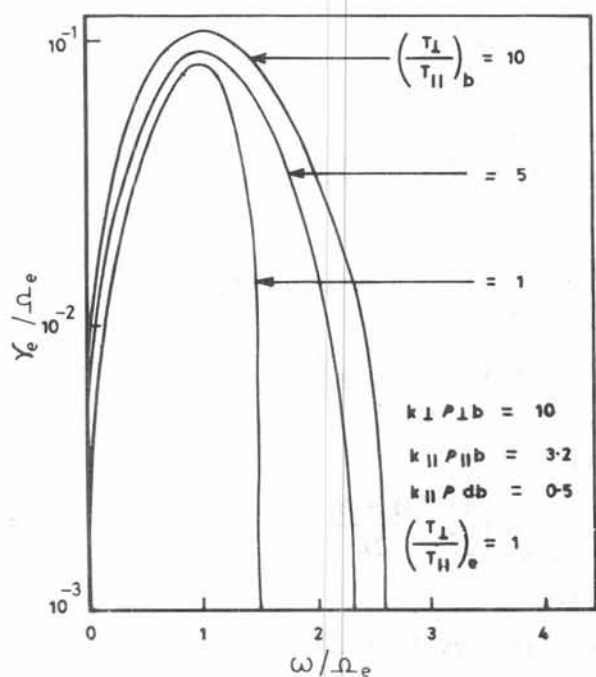


Fig. 2—Growth rate of electrostatic whistler waves

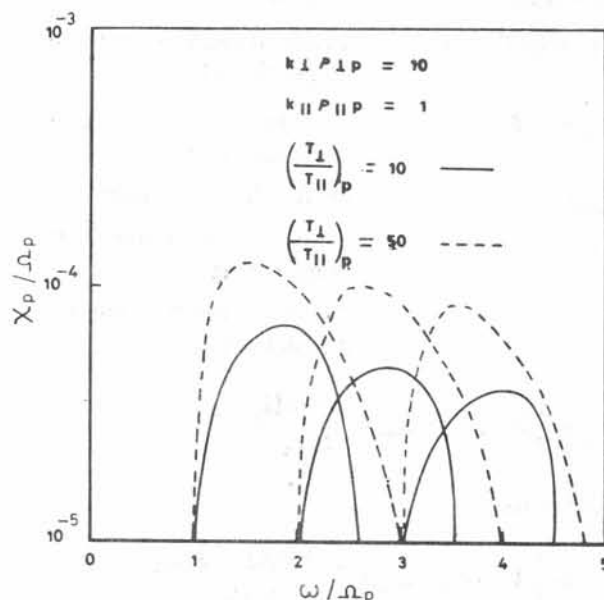


Fig. 4—Damping rate of ion-cyclotron waves

anisotropy due to protons or at  $(m + 1/2)\Omega_p$  for higher values of  $(T_{\perp}/T_{\parallel})_p$ . Since the damping occurs either at harmonics or at half harmonics of the proton-cyclotron frequencies, the occurrence of the attenuation bands as shown in Fig. 3 may be interpreted in terms of the damping rate of ICH wave at the local proton-cyclotron frequency.

#### Acknowledgement

One of the authors (A K G) acknowledges the Natural Sciences and Engineering Research Council (N S E R C) of Canada for financial support.

#### References

- 1 Smith R L, *Nature (GB)*, 224 (1969) 351.
- 2 Mosier S R & Gurnett D A, *J Geophys Res (USA)*, 74 (1969) 5675.
- 3 James H G, *J Geophys Res (USA)*, 81 (1976) 501.
- 4 Yoshino T, Ozaki T & Fukunashi H, *J Geophys Res (USA)*, 86 (1981) 846.
- 5 Watanabe S, Ondoh Y, Nakamura Y & Murakami T, *Antarctic Res (Japan)*, 64 (1979) 159.
- 6 Klumper D H, *Physics Canada (Canada)*, 31 (1975) 53.
- 7 Horita R E & James H G, *J Geophys Res (USA)*, 87 (1982) 9147.
- 8 Gwal A K & Singh M, *Indian J Radio & Space Phys*, 17 (1988) 135.
- 9 Kiwamoto Y, *J Geophys Res (USA)*, 84 (1979) 462.
- 10 Ondoh T, Nakamura Y & Murakami T, *J Radio Res (Japan)*, 27 (1980) 141.
- 11 Stix T H, *The Theory of Plasma Waves* (McGraw Hill, New York), 1962, 225.
- 12 Gwal A K & Mishra K D, *IEEE Trans Plasma Sci (USA)*, 5 (1977) 146.